Sustainable Energy Technologies and Assessments 33 (2019) 14–23

Contents lists available at ScienceDirect

Sustainable Energy Technologies and Assessments

journal homepage: www.elsevier.com/locate/seta

Original article

Characteristics of halide oxidation at graphite electrode for use in halide batteries

Diego F. Quintero Pulido[a,b,*], Marnix V. ten Kortenaar[a], Johann L. Hurink[b], Gerard J.M. Smit[b]

[a] Dr Ten B.V., Rondweg 11M/N, 8091 XA Wezep, the Netherlands
[b] Faculty of Electrical Engineering Mathematics Computer Science, University of Twente, P.O. Box 217, 7500 AE Enschede, the Netherlands

ARTICLE INFO

Keywords:
Halide oxidation
Bromide
Graphite
Aqueous solution
Microgrids
Batteries

ABSTRACT

The oxidation of halides, in particular bromide, has been studied in aqueous solutions on graphite electrodes by voltammetry, electrochemical impedance spectroscopy (EIS) and UV–Vis spectroscopy in light of its application in halide/halogen batteries used in microgrids. Voltammetry indicates fairly large differences in potentials and current density between different halide salts, concentrations, cation type and pH. Also, oxidation kinetics in 7MNaBr were much higher than in 7M$ZnBr_2$ solutions while no large differences were observed between these solutions at 2 M. This may be related to the effect that positive ions (Na^+ and Zn^+) may have an influence in halide oxidation kinetics at the large positive electrode potentials which indicated that local ionic potential effects affect the oxidation rate of the reaction. Moreover, EIS spectra seemed to go in line with this view, as there was a large resistance between $ZnBr_2$ and NaBr in the electrolyte phase transfer element. This difference is possibly related to different polybromide formation rates (for the reaction $Br^- \rightarrow Br_x^-$ + xe-). Additionally, results and literature shows that all data may be fitted by one equivalent circuit with the fitted circuit and Nyquist plots showing the complexity of the reaction by the presence of different resistors and capacitors.

Introduction

Batteries are an appealing technology that can be used as an alternative for managing the increase of electricity in both buildings and households [1–3]. Recent advances in halide carbon based battery technologies have increased the potential to create off-grid households [4]. Furthermore, the combination of renewable energies with these new batteries used within microgrids is under simulation by the University of Twente in the Netherlands [5–7]. However, an actual large scale application of batteries goes along with a detailed understanding of reliability, power behavior, electrochemical and chemical properties. In this paper, the last two aspects are addressed, whereby a focus is on a detail description of the bromide (Br-) oxidation at graphite electrode.

Current battery technologies are still unable to approximate to the max energy capacity of the halide/halogen redox couple. This is due to problems with ion solubility and the complex halide reaction mechanisms [8]. However, halide compounds such as: chloride, iodide, and bromide have attractive electrochemical properties, for instance, moderate theoretical standard reduction potential (Cl^- 1.358 V, I^- 0.53 V and Br^- 1.066 V) and good theoretical specific energy and power [9,10]. Compared with electrochemical studies performed with halides such as chloride and iodine, less can be found in literature on the kinetics and mechanism of bromide oxidation, e.g. at graphite (which is the most common electrode in halide batteries). Most of the work found about bromide electrochemistry has been done for the development of the zinc bromide flow battery [11–14], also as an alternative for the cathode material in the vanadium flow battery [15] and polysulphide flow battery [16]. In these technologies, the bromide oxidation operates in a complexed chemical bond with ammonium morpholine compounds. This to some extent, prevents halide/halogen recombination and reduces its volatility nature [17].

The mechanisms of the bromide oxidation without complexing agents are still a challenge for researchers. E.g. White [18] and Vogel [19] studied the kinetic behavior of bromide oxidation at Pt electrode. Diaz [20] researched the Br^-/Br_2 reaction and pH effect at Au electrode, Conway [21] evaluate the exchange current density and Tafel behavior at Pt electrode, Heintz [22] studied the bromide oxidation concentration effect using cation membranes and Pell [23], investigated the bromide oxidation at low-temperature on carbon electrodes. Other work has been recently done by Walter [24] using carbon nanotubes and carbon cryogels electrodes. From these studies three main aspects can be concluded: First, in voltammetry it is possible to

* Corresponding author at: Faculty of Electrical Engineering Mathematics Computer Science, University of Twente, P.O. Box 217, 7500 AE Enschede, the Netherlands.
E-mail address: d.f.quinteropulido@utwente.nl (D.F. Quintero Pulido).

https://doi.org/10.1016/j.seta.2019.03.001
Received 13 February 2018; Accepted 4 March 2019

observe two electrochemical processes that govern the halide reaction, one when the halide is oxidase showing a linear increase in the current density and another when the halogen is reduce showing a clear wave. These processes include the step formation of the trihalide/polihalide ions in an aqueous solution which leads to a semi-reversible redox reaction. The mentioned results were observed first by Faita [25] and supported recently by other authors for the halide water system [18,26]. Furthermore, the halide oxidation is a multistep process in which the increase in current may correspond to the oxidation of polybromides (Br_x^-) in the form of Br^- - Br_x^- and of Br_x^- - Br_2^- this was observed more clear using nitrobenzene as supported solution in $ZnBr_2$ electrolyte [27]. Finally, the studies of the halide oxidation have in common the use of a metal halide salt (e.g. $ZnBr_2$, NaBr and KBr) in an aqueous solution, which has implications in the aqueous form of the halide bond to the cation in which the halide-cation exist in balance in the form of e.g $Zn_{x+y}Br_{x+y}^-$ [28,29].

In this research, we study the kinetics and mechanism that rule the bromide oxidation at graphite electrode in an aqueous solution in conditions as close as possible to practical batteries. The reason for this is that we want to get a better understanding of the electrochemical processes that occur in halide batteries, which are relevant for large scale implementation in microgrids. This paper is organized as follows: First, a cyclic voltammetry (CV) analysis is presented for different concentrations of halide salts and a detail comparison of $ZnBr_2$ and NaBr aqueous solutions is given. Further, it is showed an electrochemical impedance spectroscopy (EIS) analysis using a circuit fitting procedure and Kramers-Kronig (KK) transform validation method proposed by Boukamp [30,31]. Lastly, the paper addresses UV–Vis spectra results to analyze further the studied aqueous solutions.

Experimental methods

The reagents

$ZnBr_2$ puriss anhydrous, ≥98%, Br_2 reagent grade, $ZnCl_2$ ACS reagent, ≥97%, ZnI_2 purum p.a., ≥98.0% (AT), NaBr ReagentPlus®, ≥99%, HCl ACS reagent, 37%, and NaOH reagent grade, ≥98%, pellets all from Sigma Aldrich were used with not further purification.

The equipment

The cyclic voltammetry-chronoamperometry experiments were performed with a PGSTAT 101 compact unit from the company Metrohm Autolab. The pH and temperature were recorded with a Hanna HI 9811-5. The impedance spectroscopy measurements were performed with a Model 600E Series Electrochemical Analyzer from the company CH instruments.

Voltammetry analysis

Fig. 1 shows the electrochemical cell used for this work. Graphite was the working and counter electrode, the sizes of the electrodes were 3 mm and 20 mm diameter respectively. The experiments were performed with Ag/AgCl as reference electrode. The working, counter and references electrode were immersed in 20 ml of electrolyte solution. The graphite was washed and polished with alumina paper caliber 15 after every single experiment. The experiments were performed in different aqueous solutions, with a scan rate of 100 mV/s, in a potential window from −1.2 V to 1.9 V.

The EIS analysis

EIS analysis was done with the EIS fitting procedure in which the elements are analysed with the software-method EQUIVCRT developed by Boukamp [30,32,33]. This method provides more information into the kinetics of the reaction, and can be also validated by a linear KK transform test method developed by the same author [31].

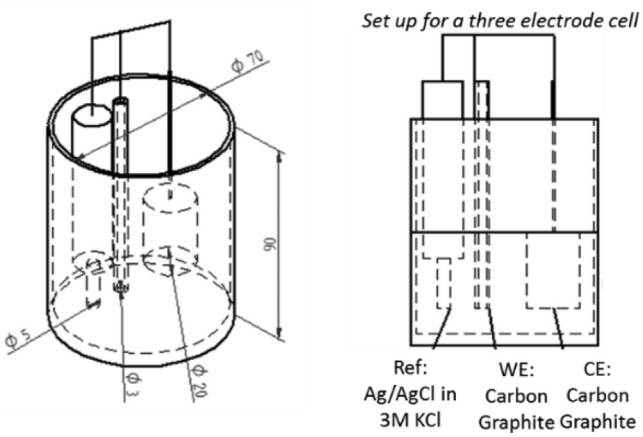

Fig. 1. The electrochemical cell.

Results and discussion

Halide oxidation reaction

CV experiments were conducted to gain an insight into the difference between halide oxidation at graphite in aqueous solution, the studied ions were Cl^-, I^- and Br^-. The analysis was performed using different halide compounds (2 M $ZnBr_2$, 2 M NaBr, 2 M ZnI_2, and 2 M $ZnCl_2$). Fig. 2a shows that the halide voltammograms have a similar shape between 0 V and 1.9 V. In detail, when a potential was applied to the electrochemical cell a current respond was obtained, stripping the potential until a value of 1.9 V showing linear behaviour, then the potential was reversed and the current reduces thus starting the reduction reaction. Here, all the studied halides defined a clear wave with peaks at different potentials. The peak potential depends on the studied halide thus varying the current density. This effect is may be related to the halide/halogen electrochemical reduction potential which varies between the different halide ions (E^o = Cl^- 1.358 V, Br^- 1.066 V and I^- 0.53 V) and also may be affected by processes at the electrode that affect the current density responds e.g. diffusion, side reactions and intercalation. This observations were also presented by the research performed by Arai [34] and Chen [35].

Between 0 V to −1.3 V was observed a change in the voltammogram shape. This change is possibly related to the zinc deposition/reduction reaction at graphite electrode, which occurs in a two steps process defining two peaks. The deeper study of the zinc reaction is beyond the scope of this study. However, the zinc reaction was included in the voltammetry in order to show the active presence of the ions in the studied halide compounds and to keep our research as close as possible to real battery processes that could affect the halide oxidation.

A comparison between $ZnBr_2$ and NaBr at two different concentrations (2 M and 7 M) is shown in Fig. 2b and c respectively. The voltammetry shows that although $ZnBr_2$ and NaBr had same anion, the voltammetry potential and current density were different at 2 M (Fig. 2b) and the difference is greater at 7 M (Fig. 2c). Table 1 presents a comparison of the current density at 1.5 V in the different halide oxidized at graphite in aqueous solution. The 2 M $ZnBr_2$ and 2 M ZnI_2 have the highest current density in comparison with 2 M $ZnCl_2$ and 2 M NaBr. However, the current density in 7 M $ZnBr_2$ (148 mA cm^{-2}) is lower than at 2 M (243 mA cm^{-2}). On the contrary 7 M NaBr has a higher current density than 2 M NaBr aqueous solution. This effect is observed in more detail in the voltammetry when the $ZnBr_2$ and NaBr are scanned at different concentrations (Fig. 3).

When comparing in detail the effect of the Br- oxidation in the voltammetry at 1.5 V between the $ZnBr_2$ and the NaBr (see Fig. 4). It is

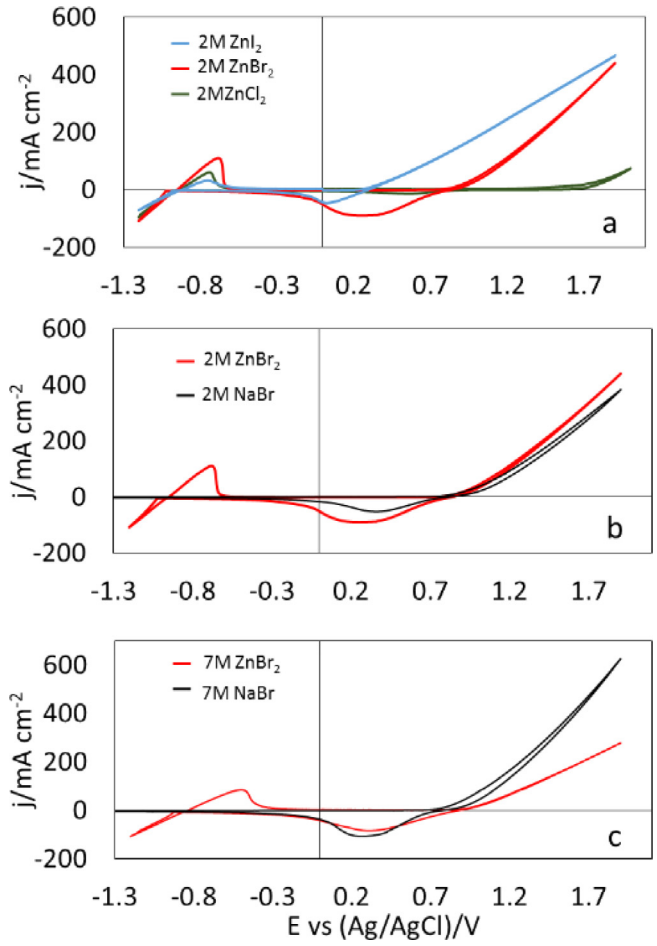

Fig. 2. Cyclic voltammetry of graphite in aqueous solutions at 100 mV/s and Ag/AgCl reference electrode of a) 2 M $ZnBr_2$, 2 M ZnI_2 and 2 M $ZnCl_2$ b) 2 M NaBr and 2 M $ZnBr_2$ and c) 7 M $ZnBr_2$ and 7 M NaBr.

Table 1
Current density from CV experiments at 1.5 V of different metal halides.

Metal Halide	1.5 V mA cm^{-2}
2 M $ZnBr_2$	243
2 M ZnI_2	359
2 M NaBr	215
2 M $ZnCl_2$	11.5
7 M $ZnBr_2$	148
7 M NaBr	346

observed that in the $ZnBr_2$ aqueous solutions the Br- oxidation current density tends to increase gradually until a concentration of 2.5 M, reaching a value of 259 mA cm^{-2}. Then, it decreases progressively until 28 mA cm^{-2} at a concentration of 14.5 M. In the case of NaBr, the Br- oxidation current density in the voltammetry at 1.5 V increases constantly until a value of 320 mA cm^{-2} at a concentration of 7 M (point in which no more NaBr was possible to be dissolved at room temperature). The current density increases proportional to the concentration of the solution, thereby behaving in correlation with the Randles-Sevcik approach (Eq. (1)). In which; i_p is the current density, n is the number of electrons, A is the electrode area, F is the faraday constant, D is the diffusion coefficient, C is the concentration and ν is the scan rate.

$$I_p = (2.6 * 10^5) n^{3/2} A C D^{1/2} v^{1/2} \quad (1)$$

Another difference observed between $ZnBr_2$ and NaBr aqueous

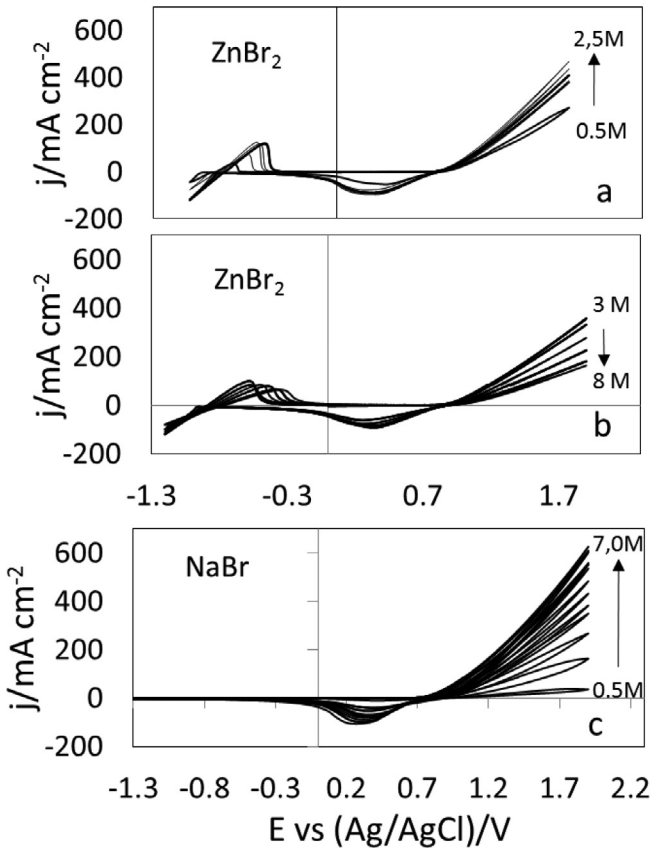

Fig. 3. Cyclic voltammetry of graphite at different concentrations of $ZnBr_2$ and NaBr in aqueous solutions at 100 mV/s and Ag/AgCl reference electrode of: a) Concentration from 0.5 M to 2.5 M of $ZnBr_2$, b) Concentration from 3 M to 8 M of $ZnBr_2$ and c) Concentration from 0.5 M to 8 M of NaBr.

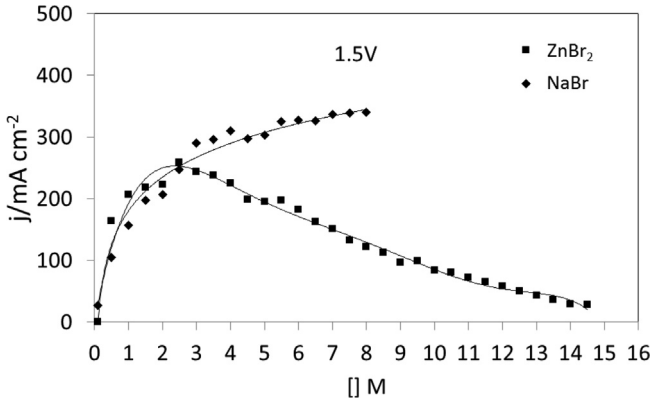

Fig. 4. Current density at 1.5 V of graphite at different concentrations of $ZnBr_2$ and NaBr in aqueous solutions at 100 mV/s and Ag/AgCl reference electrode.

solutions is in the pH. Fig. 5 shows the pH vs concentration effect of $ZnBr_2$ and NaBr in aqueous solution, in the case of the $ZnBr_2$ the pH decreases when the concentration increases and at the maximum concentration (14.5 M) the pH value is 0.2. In the case of NaBr, the pH vs concentration experiment showed a slightly increase from 7.0 (at 0.1 M) to 8.5 (at 7 M). The changes observed during the voltammetry and pH experiments showed that there is an interesting difference between bromide oxidation and the rest of the halide oxidation reactions and that depending on the studied halide the reaction kinetics differs. In this paper, we elucidate deeper in the analysis of the bromide oxidation reaction by studying the mechanism of the reaction at graphite electrode using $ZnBr_2$ and NaBr to show a comparative analysis.

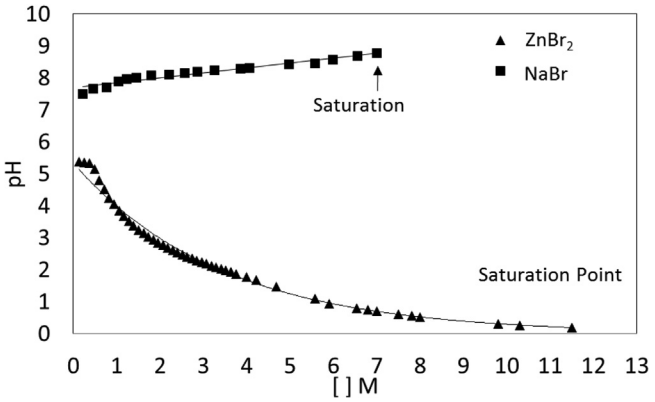

Fig. 5. Effect of pH on concentration on $ZnBr_2$ and NaBr aqueous solution.

Halide oxidation at graphite in $ZnBr_2$ and NaBr aqueous solutions

In this section it is described the possible processes that maybe involve in the bromide oxidation voltammetry presented in Section "Halide oxidation reaction". Here, it is explained three different physical and chemical processes that may affect the kinetics of the halide oxidation: The aqueous crystal structure of $ZnBr_2$ and NaBr in aqueous solutions, the formation of the tribromide/polibromide species and intercalated bromine into graphite electrode.

The aqueous crystal structure of $ZnBr_2$ and NaBr in aqueous solutions

One possible explanation for the oxidation behaviour of Br- in aqueous solution is its crystal structure which is different for $ZnBr_2$ and NaBr. In the case of $ZnBr_2$, Duvlet [28] proposed that there are two different kinds of Zn atoms in the crystal structure of $ZnBr_2$ solutions. The first Zn atom is a tetrahedral coordinated by four Br atoms this forms dimeric $Zn_2Br_6^{2-}$ groups with mmm crystallographic symmetry. The bridging function of Br distorts both the bond distances and the angles around Zn from an ideal tetrahedron. The second Zn atom forms $Zn(H_2O)_6^{2+}$ octahedral also with crystallographic mmm symmetry.

These are linked to the $Zn_2Br_6^{2-}$ groups through of O–H^+…Br^- hydrogen bonds to form infinite chains of $[Zn(H_20)_6]^{2+}$- $[Zn_2Br_6]^{2-}$ extended along and through O–H^+…Br^- hydrogen bonds into layers. Later research developed by Simonet[36] suggest that both Zn and Br ions are largely hydrated under normal conditions in aqueous solutions and that Zn–Br pairs are formed in hydrothermal conditions. This is related to the octahedral-to-tetrahedral evolution of the Zn local environment, where the majority of Zn atoms are surrounded by - water octahedral in normal conditions and by distorted tetrahedral involving Br and O atoms in hydrothermal conditions. The two explanations for $ZnBr_2$ crystal structure showed that, the halide oxidation may be influenced by the bonds of Zn and Br atoms which at high molar concentration (7 M), are influence by Zn O^- H^+ in their crystal forms in aqueous solutions which may slow down the kinetics of the Br species towards the graphite electrode thus possibly reducing its current output. In the case of NaBr, Omta[37] and later studies by Lin [38] showed that the average of hydrogen and oxygen molecules surrounded the Na^+ and Br^- in aqueous solutions have the same number compared with pure water in low concentrations and that increasing the NaBr concentration only affects slightly the bond of Na^+ Br^- thus not creating infinite chains in the solution (like in the case of $ZnBr_2$). This behavior suggest that Br- ions can move faster in NaBr aqueous solutions and the halide oxidation may occur at a faster rate than in $ZnBr_2$ aqueous solutions thus possibly explaining the effect in current density at higher concentrations (e.g. 7 M), observed in Figs. 3 and 4.

The formation of the tribromide and polibromide species in aqueous solution

Another important aspect that may influence the Br- oxidation reaction is the formation of tribromide and polibromide. In literature is found information of the Br- oxidized form e.g. Adanuvor and White [39] researched the formation of the tribromide complex base on the step reaction proposed first by the Volmer-Heyrovsky (V-H) discharge desorption mechanism equation for Br- oxidation (Eqs. (2) and (3) respectively). The Br^- ions are present in the solution and are adsorbed during the oxidation process (Eq. (2)) creating bromide adsorbed ($Br\text{-}_{ads}$), a second reaction step occurs when the Br_{ads}^- oxidases at the electrode surface in the presence of Br- forming Br_2 (Eq. (3)). A third chemical reaction step occurs after the charge transfer, when Br_2 is in contact with the remaining Br- ions forming the tribromide complexation (Br_3) (Eq (4)), which has been studied in detail by different authors [21,40]. The chemical oxidation reaction is a series of continues processes between the new form element (Br_2, Br_3) with Br- ions forming different types of polybromides complexes (Br_x) (Eq. (5)) this effect is observed in more detail when using complexing agents. This type of mechanism of the Br- oxidation reaction has been studied in detail recently by Park [41]. Park, concluded that the Br- electrochemical oxidation is a reaction that occurs with Br^- transfer-water step. This possibly occurring before (re)combining with other species in the aqueous environment, and this difference is relative to the current density and the concentration of Br^- ions in the electrolyte.

$$Br^- \rightarrow Br_{ads}^- + e^-(V) \quad (2)$$

$$Br{-}_{ads} + Br^- \rightarrow Br_2 + e{-}\ (H) \quad (3)$$

$$Br_2 + Br^- \rightarrow Br_3 \quad (4)$$

$$Br_3 + Br - \rightarrow Br_x \quad (5)$$

Intercalated bromine

During the performed experiments on halide oxidation, it was used graphite as working electrode. In this case, it is possible that Br_2 intercalation may contribute in the varying current density of the Br- oxidation in aqueous solution. In literature, e.g. Izumi [42] researched the electrochemical intercalation of Br_2 into graphite in aqueous solutions, in the study was observed that Br- oxidation reaction at different concentrations had an effect in the current density during voltammetry studies. Izumi, concludes that the effect is related to the formation of intercalated Br_2 into the graphite electrode, this effect is supported by changes in electrode weight and decrease in relative electrical resistivity. Later studies by Gaier [43] who studied the aqueous electrochemical intercalation of Br_2 into graphite fibers, showed that the effect observed in the graphite electrode was similar for carbon fibers. The mechanism to create intercalated Br_2 are related to the concentration of the halogen during the oxidation reaction near the graphite electrode. This effect was observed in temperatures from 5 °C to 40 °C. The observations by Izumi and Gaier are in accordance with the voltammetry recorded in this research for Br- oxidation at graphite (Figs. 3 and 4), showing that graphite may have a contribution in the kinetics of the Br- oxidation.

The three effects that are described before as a possible cause of kinetic changes during voltammetry for the Br- oxidation in aqueous solutions at graphite electrode, were studied using electrochemical impedance spectroscopy (EIS). This in order to observe if the Br- oxidation at carbon graphite may be represented with an electrical circuit which may give an indication of the contributions of each step in the oxidation reaction. The presence of the elements in the EIS study are only analyze by the presence of capacitor and resistances observed and not by other spectrometry methods. The analysis is performed using $ZnBr_2$ and NaBr for comparison purposes base on the differences observed in the cyclic voltammetry in Figs. 3 and 4.

EIS analysis of bromide oxidation at graphite:

The EIS analysis was performed in different steps: First, a plausible reaction pathway is taken from literature and a possible reaction model

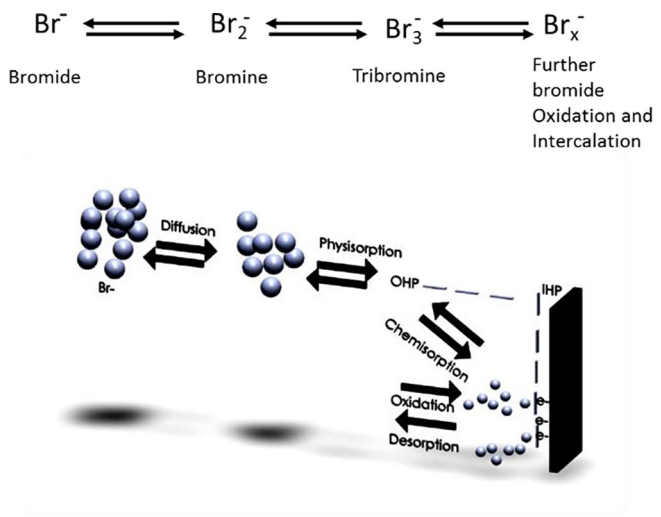

Fig. 6. Reaction representation of bromide oxidation pathway at graphite.

is created. Second, an expected circuit is drawn based on the assumption of the model for the reaction. Third, the circuit is compared against the lab results using the EQUIVCRT software and fourth the circuits are analysed with the KK transform test.

Expected circuit

The Br- oxidation reaction pathway at graphite considered for the analysis in EIS is shown in Fig. 6a and b. Base on this, from the Br- oxidation reaction equation an expected equivalent circuit was derived (Fig. 7a). Taking into account that each reaction step has a sub-analogue electrical element. First, we considered the chemical reaction that is shown in Fig. 6b in which diffusion of Br^- ions is followed by physisorption in the outer Helmholtz plane (IHP). It is also possibly observed chemisorption processes presented in parallel to the double layer capacitance in the inner Helmholtz plane (IHP) and various Br^- ions may be captured close to the electrode (oxidation-desorption) forming Br_2 and later the Br_3. The oxidation process will continue forming Br_x and possibly intercalated graphite with Br_2, Br_3, and Br_x close to the

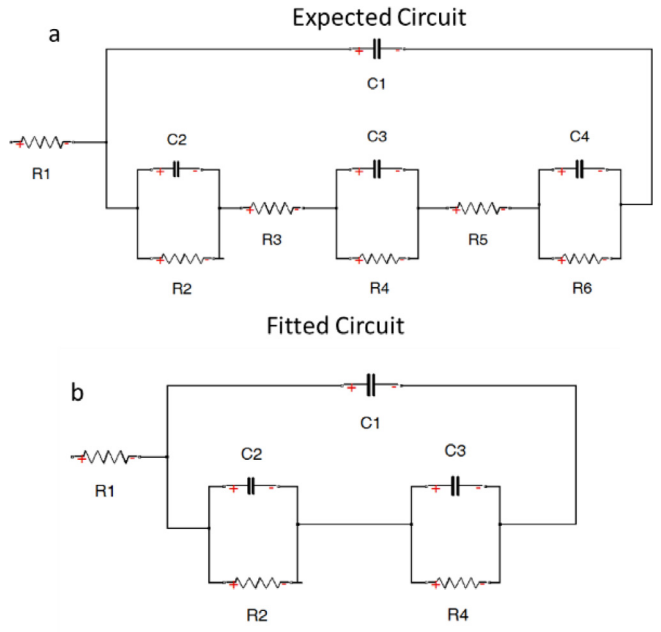

Fig. 7. Equivalent circuits for the bromide oxidation at graphite electrode with EIS software EQUIVCRT a) Expected circuit and b) Fitted circuit.

electrode. The different sets of capacitors and resistor in Fig. 7b were designed base on the previous analysis of the Br- oxidation reaction (see Section "Halide oxidation at graphite in $ZnBr_2$ and NaBr aqueous solutions"). It is assumed that each pair of capacitor-resistance may represented one of the steps in the reaction. Furthermore after the expected circuit was designed it was tested in the EQUIVCRT in order to observe if the circuit fits the recorded data of impedance.

Fitted circuit

The fitting of the circuit is a process based on the assumption that one particular circuit may fit (or mimic) all data that was found in the impedance measurements. First the impedance data is recorded. For this, the impedance data was collected at four different potentials 0 V, 0.5 V, 1 V and 1.5 V that are in relation with the voltammetry of Br- oxidation at graphite presented previously in Figs. 3 and 4.

We first tested the expected circuit (Fig. 7a) and we notice that it does not fit completely the data given. The software EQUIVCRT test the data with the given circuit and start to iterate until finding the best match for the recorded data. After testing with over 25 circuits, one circuit seems to fit well the entire data at the studied potentials. In principal, some of the resistance and the diffusion elements are merged from the expected circuit, this might be due to the low influence in the frequency studied or do to extreme low noise in the system. The resulting circuit is shown in Fig. 7b. The spectra had an X^2 value of 10^{-3} or 10^{-4} (see Table 2). (The X^2 value represents the residuals of the correlation of data with the electrical propose system. The X^2 results are explained in more detail in Section "Spectra analysis"). The X^2 values are expected to be as close to zero as possible. Although, the resulting X^2 values are large, the circuit mimics reasonably the recorded impedance data and it is in line with our comprehension of the Br- oxidation reaction. Therefore, the fitted results were further analysed using the different concentrations of NaBr and $ZnBr_2$.

Spectra analysis

As shown in the voltammetry of Br- oxidation at graphite in aqueous solutions of NaBr and $ZnBr_2$ (Figs. 3 and 4). There is a difference in the voltammetry when the concentration of the electrolyte is change. The difference is more notorious at a concentration of 7 M and at 2 M. Due to this observation, the analysis of this effect in both salts NaBr and $ZnBr_2$ was studied in more detail using EIS. Fig. 8a shows the impedance spectra of 7 M $ZnBr_2$ and 7 M NaBr at graphite electrode, with the real and fitted data at different positive potentials (0 V, 0.5 V, 1 V and 1.5 V) together with the steady state current in the region of −0.2 V to 1.8 V. Region in which, Br- oxidation is possibly occurring. In detail, at the concentration of 7 M in both $ZnBr_2$ and NaBr there was not substantial change in the impedance spectra at the potential of 0 V and 0.5 V. However, when the impedance test was performed at 1 V and 1.5 V the spectra had a different shape, showing at 1 V two clear loops and at 1.5 V one large loop with a vending loop at higher frequencies. The changes in the impedance spectra are possibly related to the standard redox potential of Br- reaction which in literature and in our study is observed at potentials about 0.9 V.

Moreover, the impedance in the 7 M $ZnBr_2$ was overall larger than in the 7 M NaBr aqueous solutions at the potential of 1.0 V and 1.5 V. This impedance behaviour may be related to the changes observed in the voltammetry where the current density recorded is lower in 7 M $ZnBr_2$ than in 7 M NaBr and also to the different pH of the solution as shown in Fig. 5. Previous test performed by Jeffrey[44] support our results, showing that Br- oxidation in NaBr aqueous solutions at different concentrations may have an effect in the kinetics of the reaction and in the pH of the solution.

On the other hand, the impedance spectra in 2 M $ZnBr_2$ and 2 M NaBr has a different behaviour than at 7 M. Fig. 9 shows the impedance spectra analysis at different positive potentials (0 V, 0.5 V, 1.0 V and 1.5 V) in 2 M $ZnBr_2$ and 2 M NaBr aqueous solutions at graphite electrode. In this case, during both experiments the impedance spectra

Table 2
Circuit fitted values for the Impedance spectra of 7 M, 2 M $ZnBr_2$ and 7 M, 2 M NaBr.

	V (V)	R1 (Ω)	C 1(F)	R2(Ω)	C2 (F)	R3(Ω)	C3(F)	X^2
7 M NaBr	0	4.47E + 00	4.70E2 − 08	1.09E + 02	2.53E − 05	3.89E + 01	2.04E − 04	6.56E − 04
	0.5	4.31E + 00	7.14E − 08	5.47E + 01	2.22E − 05	6.42E + 01	1.22E − 04	1.03E − 03
	1	3.54E + 00	2.09E − 07	9.68E + 01	1.91E − 06	4.03E + 01	1.71E − 04	7.50E − 04
	1.5	3.51E + 00	2.83E − 07	9.35E + 11	6.72E − 13	2.04E + 01	1.71E − 04	6.12E − 04
7 M $ZnBr_2$	0	8.55E + 00	4.82E − 08	9.55E + 01	4.80E − 05	−2.57E + 14	2.60E − 14	9.33E − 04
	0.5	8.23E + 00	5.56E − 08	9.26E + 01	5.11E − 05	2.05E + 13	1.42E − 14	5.69E − 04
	1	9.32E + 00	2.47E − 08	1.19E + 03	4.01E − 07	5.82E + 02	1.49E − 06	3.46E − 04
	1.5	9.47E + 00	2.73E − 08	8.51E + 02	9.32E − 07	7.16E + 11	−2.06E − 12	2.46E − 04
2 M NaBr	0	4.45E + 00	8.51E − 08	2.23E + 02	2.77E − 05	5.12E + 01	1.47E − 05	5.28E − 04
	0.5	5.33E + 00	5.18E − 08	2.53E + 02	1.86E − 05	5.02E + 01	1.34E − 05	1.11E − 03
	1	4.99E + 00	6.88E − 08	1.55E + 03	−8.58E − 04	4.06E + 01	2.50E − 05	1.29E − 03
	1.5	2.77E + 01	2.68E + 00	−4.55E + 01	1.62E − 02	3.17E + 11	3.63E − 14	2.52E − 04
2 M $ZnBr_2$	0	5.14E + 00	7.97E − 08	3.94E + 02	1.61E − 05	5.93E + 01	2.34E − 05	5.77E − 04
	0.5	5.49E + 00	5.55E − 08	1.30E + 03	8.61E − 07	3.87E + 01	3.21E − 05	9.50E − 04
	1	5.34E + 00	5.63E − 08	2.54E + 02	1.53E − 01	3.52E + 01	6.91E − 05	6.26E − 04
	1.5	4.18E + 00	2.59E − 07	3.13E + 01	7.92E + 00	4.03E + 03	1.49E − 13	2.16E − 04

shape shows a similar behaviour. Here, it is not observed changes in the spectra at potentials of 0 V and 0.5 V. However, the spectra change when the potential is increase to 1 V showing two semicircles and one semicircle at 1.5 V (this observation is also similar when testing 7 M $ZnBr_2$ and 7 M NaBr). At 1 V the impedance spectra shape maybe a representation of the Br- oxidation reaction as observed previously in Fig. 8. In this case, it is observed that the impedance is larger in the 2 M $ZnBr_2$ than in the 2 M NaBr aqueous solution. Furthermore, at the potential of 1.5 V the impedance is larger in the 2 M NaBr than on the 2 M $ZnBr_2$. Also, the values of impedance are lower when they are tested at 1.5 V than at 1 V. These effects in the impedance spectra maybe and effect of the Br- oxidation reaction which like in the 7 M solutions occur at potentials higher than 1 V. In order to verify the reliability of the impedance data, the relative residuals are plotted in Figs. 8b and 9b. The data was calculated using the Eq. (6).

$$\Delta_{re,i} = X_{re,i} - X_{re}(w_i)/|X(w_i)| \text{ and}$$
$$\Delta_{re,i} = X_{im,i} - X_{im}(w_i)/|X(w_i)| \quad (6)$$

Here, $X_{re,i}$ and $X_{im,i}$ are the real and imaginary parts of the impedance at a data point (i), $X_{re}(w_i)$, $X_{im}(w_i)$ are the real and imaginary parts of the modelling function for w_i. The $|X(w_i)|$ is the vector length expressed in absolute value of the modelling function (X can also represent the statistical behaviour of the correlation for fitted data in the circuit). The residuals showed a trend that is closer to values between 0 and 1% for the error in the data fitting, showing that the data in the fitting correlation has a low error percentage in all the applied potentials.

As explained in Section "Fitted circuit" one single circuit fitted all the impedance spectra shown in Figs. 8 and 9. The result values of resistors and capacitors at different potentials is shown in Table 2. In general, when the potential is increase the fitted elements change proportional. The first resistance (R1) is the largest resistance due to the

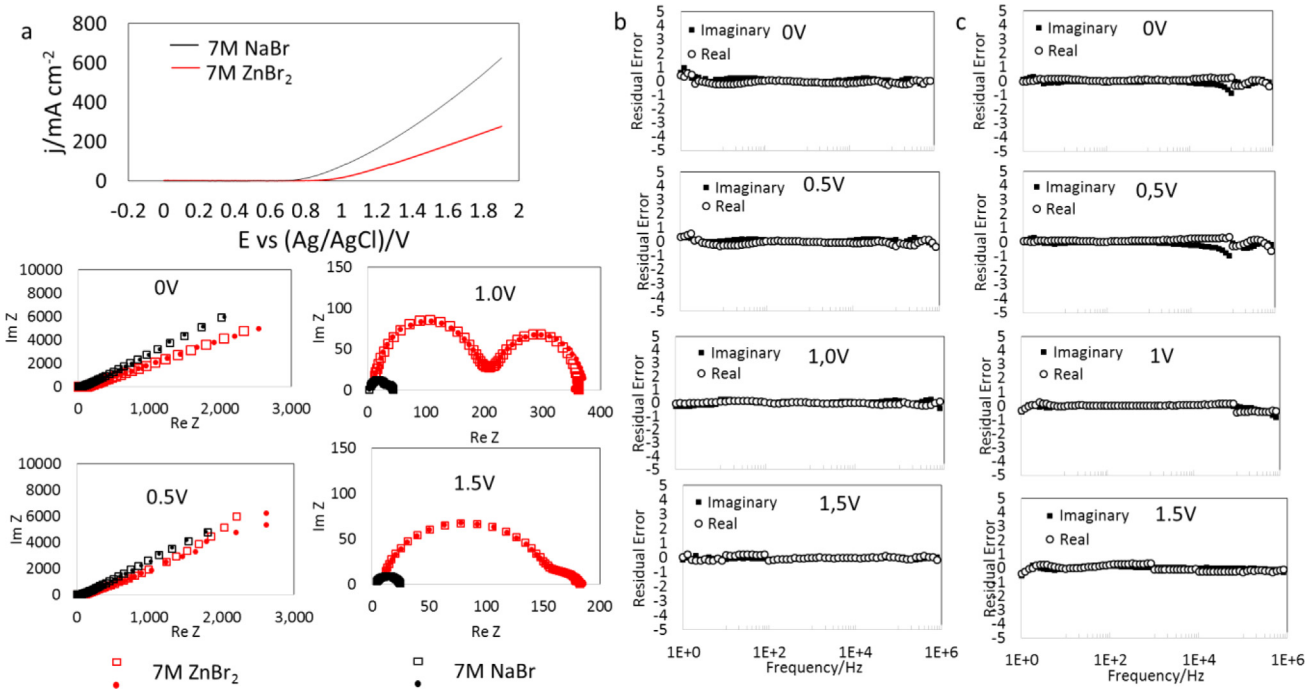

Fig. 8. a) Impedance spectra real (*) and fitted data(□) at different positive potentials together with the steady state current from graphite CV experiments on 7 M $ZnBr_2$ and 7 M NaBr, 100 mV/s and Ag/AgCl reference electrode. b) Fitted (*) and real (□) equivalent circuit frequency error 7 M $ZnBr_2$ c) fitted (*) and real (□) equivalent circuit frequency error 7 M NaBr.

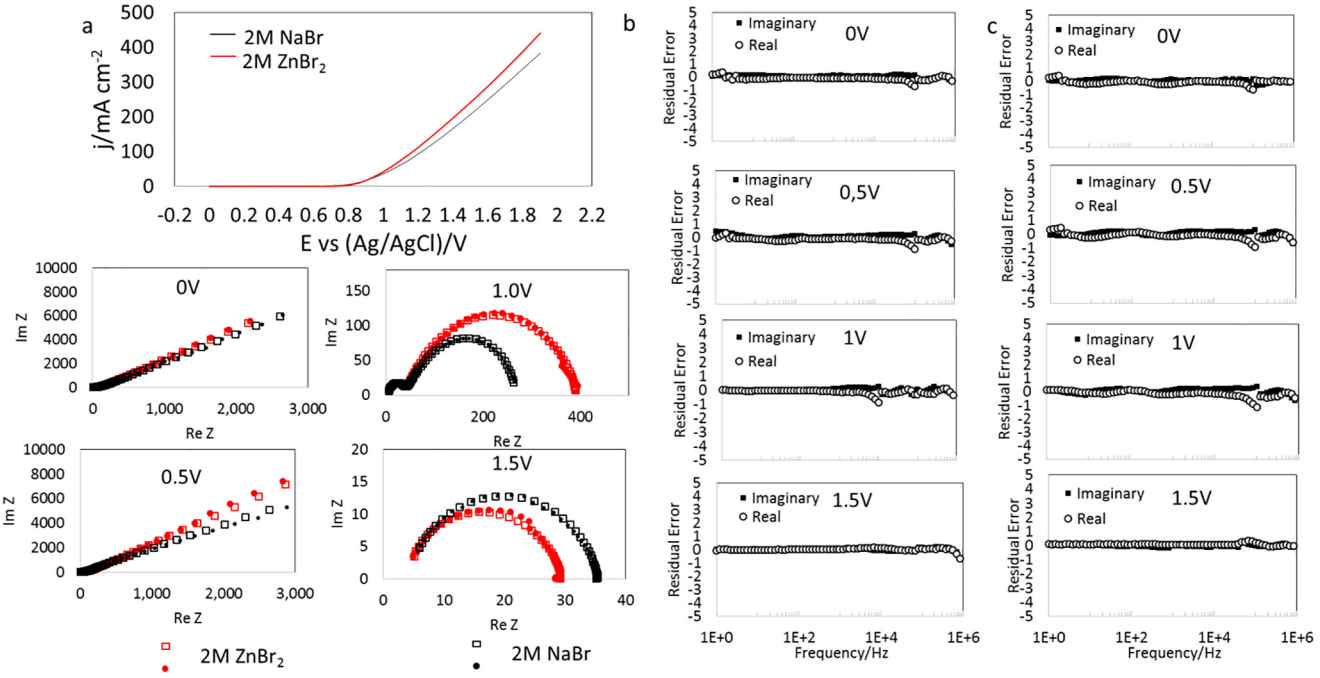

Fig. 9. a) Impedance spectra real (*) and fitted data(□) at different positive potentials together with the steady state current from graphite CV experiments on 2 M $ZnBr_2$ and 2 M NaBr, 100 mV/s and Ag/AgCl reference electrode. b)) fitted (*) and real (□) equivalent circuit frequency error 2 M $ZnBr_2$ c) fitted (*) and real (□) equivalent circuit frequency error 2 M NaBr.

distance of the particles that need to travel to the graphite electrode double layer.

The first capacitor (C1) is possibly representing the double layer capacitance, which has approximately the same value at all the potentials. The double layer capacitance is connected together with two sets of resistances-capacitors that are in series (R2C1 and R3C2). This set of resistor and capacitor may represent steps that occur in the Br- oxidation reaction. However, it is not possible by means of impedance to known the precise reaction that is occurring. Nevertheless, our impedance measurements and fitted circuit shown that there are two main reactions occurring in the Br- oxidation at graphite possibly related to the effect of Na^+ and Zn^+ in the solution, the presence of Br_2, Br_3, Br_x. and the effect of intercalation as explained in Section "Halide oxidation at graphite in $ZnBr_2$ and NaBr aqueous solutions. Furthermore, it is observe that the capacitors and resistors have different values in the tested electrolytes at different concentrations and this differences are more notorious in the potential of 1.5 V (see Table 2). Fig. 10 has been constructed in order to elucidate this effect in more detail. Here, it is shown a comparison of the fitted values for capacitors and resistors at 1.5 V in high (7 M) and low (2 M) concentrations of $ZnBr_2$ and NaBr.

Fig. 10a shows the capacitors in the fitted circuit in the 7 M $ZnBr_2$ and 7 M NaBr. In principal, the values of C1 and C2 in both cases are similar with values close to zero. However, the capacitor C3 has a value of 1.71E−04 F for the 7 M NaBr which is larger than in the 7 M $ZnBr_2$ with a value close to zero. Furthermore, the resistor R2 shows a higher value in the 7 NaBr than in the 7 M $ZnBr_2$ (see Fig. 10b) and the resistor R3 shows a larger value in the 7 M $ZnBr_2$ (7.16E+11 Oh) than in the 7 M NaBr (1.71E−04 Oh). The difference in the capacitors and the resistors in both electrolytes at 7 M, may be related to the presence of the ions Zn^+ and Na^+ in the oxidation reaction, and this effect is possible related to the different in kinetics depicted previously in the voltammetry in Figs. 3 and 4. On the other hand, the capacitors and resistors at a concentration of 2 M in $ZnBr_2$ and NaBr (Fig. 10c and d) shown a different behaviour than at 7 M.

In this case, the capacitor C1 has a value of 2.68E+00 F in the 2 M NaBr which is higher than in 2 M $ZnBr_2$ and the capacitors C2 and C3 which have a similar values close to zero for both electrolytes. The resistors shown that the highest resistance is in the resistor R3 in the 2 M NaBr (3.17E+11 Oh), which is larger than in the 2 M $ZnBr_2$ (4.03E+03 Oh). The difference in capacitors and resistors is possible related to effect in the voltammetry of 2 M $ZnBr_2$ and 2 M NaBr (Figs. 3 and 4) which shows a difference in the Br- oxidation current density. Our results suggest that the presence of capacitors and resistors may have a correlation in the outcome of the current density in the Br- oxidation reaction at graphite. However, this approach is only related to the presence of capacitor and resistors in the fitted circuit and the determination of the precise reaction that is ruling the Br- oxidation still needs to be tested by other in-situ spectrometric methods. In order to test that our data has a mathematical validity, the fitted circuit was tested using the KK transform test.

Data reliability

In order to validate the modelled circuit. The KK transform test was use with the method described by Boukamp [31]. Fig. 11 presents the results of the KK transform test for the impedance of graphite electrode in 7 M NaBr and 7 M $ZnBr_2$. The test shows that the data can be transformed according to KK theory thus confirming that the data has certain degree of reliability. As described before, the capacitors and the resistors presented in this studied are based on fitting and their actual presence in the reaction are not ascertained. However, based on the low frequency spectra it is possible to observe the presence of capacitors. This could imply that the processes are slow. Also, the analysis of the residual error shows that the values stay in the range between 0 and 5% and 10%, thus supporting the theory of the presence of the capacitive structures in the reaction.

UV vis analysis of charge experiments for bromide oxidation

After observing the difference between the Br- oxidation reaction at graphite in different concentrations of $ZnBr_2$ and NaBr, an experiment was designed in order to test these differences and the electrolytes were later analysed using UV Vis spectrophotometry. The spectrometry test is perform in order to observe the change in the electrolyte once the Br- oxidation reaction has occurred. The experiment was developed as follow: two different cells were built using two electrodes of graphite of

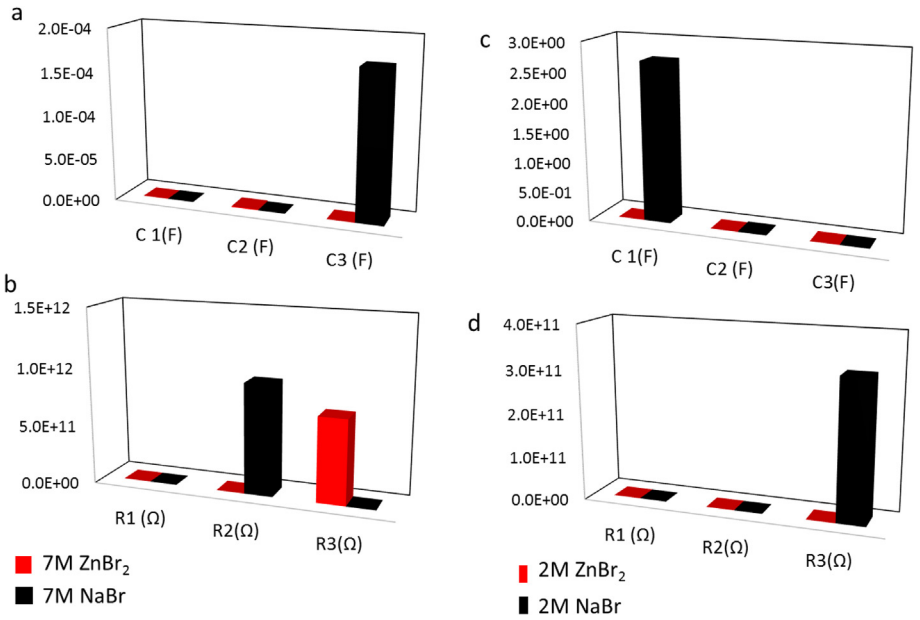

Fig. 10. Fitted circuit values at 1.5 V of a) capacitors in 7 M $ZnBr_2$ and 7 M NaBr b) Resistors in 7 M $ZnBr_2$ and 7 M NaB, c) Capacitor in 2 M $ZnBr_2$ and 2 M NaBr and d) Resistors in 2 M $ZnBr_2$ and 2 M NaBr.

20 cm^2.

The graphite electrodes were immersed in a electrochemical cell with a solution of 20 ml of 1 M $ZnBr_2$ for the first experiment and a new cell was built with 20 ml 1 M NaBr. Then, the graphite electrodes were connected as negative and positive electrode to a constant current power supply. Moreover, 100 mA constant current was used until a constant potential of 1.9 V was observed. The electrolytes were in the cell with the described conditions for 5 h. An example of the resulting electrolytes is shown in Fig. 12a, here the electrolyte changes to a light yellow colour after the experiment, which is characteristic of the Br- oxidation reaction. Moreover, UV Vis spectrophotometry was used to study the resulting electrolytes after the experiment finish. The $ZnBr_2$ and the NaBr were compared against pure Br_2 to observe the peak absorbance. Fig. 12b shows the UV Vis spectra results. The experiment was recorded from 190 nm to 1100 nm wavelength. The Br_2 shows two wavelength one at 287 nm and one at 386 nm. These peaks has been reported before by a few authors e.g Bell [43]. In his study he reported the wavelengths at 285 nm and 390 nm. These values are close to the one measured in this study. In the case of $ZnBr_2$ it is observed also two wavelengths one at 310 nm and at 386, however the second wave is less pronounce than the first wavelength. On the other hand the NaBr electrolyte shows one wavelength at 310 nm. These results suggest that there may be a difference in the UV Vis spectra between the Br_2, the $ZnBr_2$ and the NaBr electrolytes. Furthermore, the first wavelength at

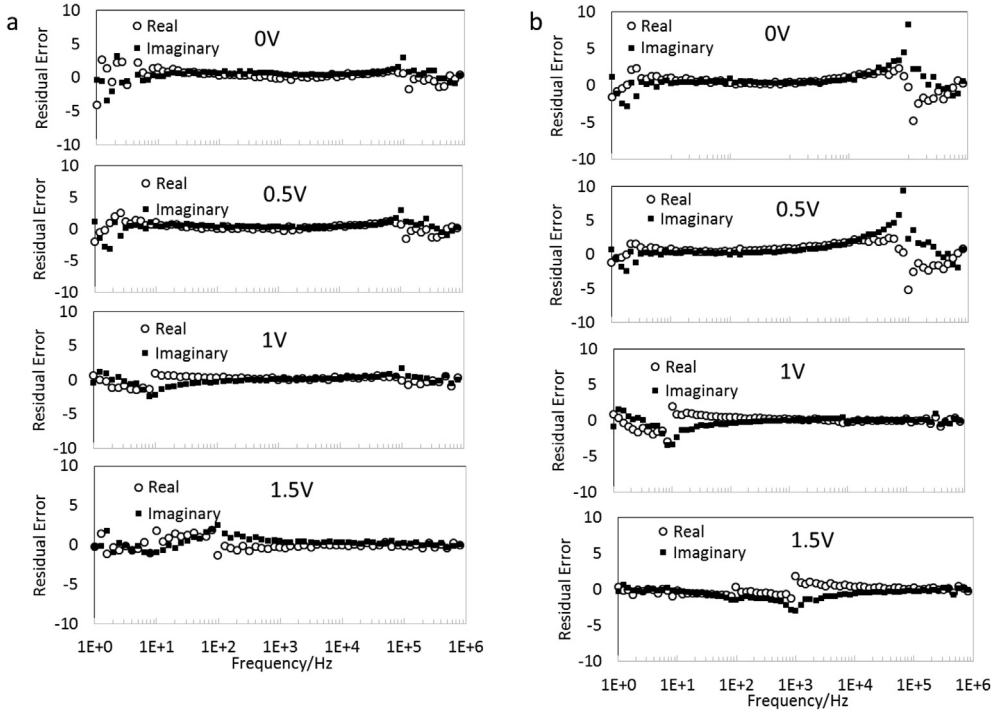

Fig. 11. KK transform analysis for experimental data of impedance measurements of Graphite electrode in a) 7M ZnBr and b) 7 M NaBr.

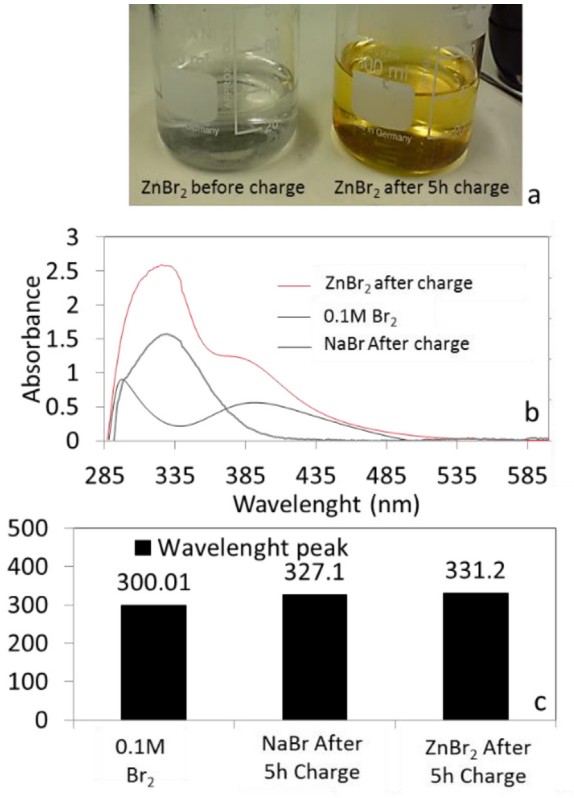

Fig. 12. a) Picture 1 M $ZnBr_2$ aqueous solution before charge and after 5 h charge at 5 mA cm^{-2} b) UV Vis spectrophotometry of 1 M $ZnBr_2$, 1 M NaBr aqueous solution charge at 5 mA cm^{-2} for 5 h and 0.1 M Br_2. c) Peak wavelength of Br_2, Charged $ZnBr_2$, and Charged NaBr.

which Br_2 is observed (280 nm) was lower than the one produced electrochemically ($ZnBr_2$ 310 nm-NaBr 310onm). And the second wavelength has a different shape in the Br_2 than in the $ZnBr_2$. Although, both wavelengths are present at close wavelength and in the case of the NaBr the second wavelength was not present.

Conclusions

The results with cyclic voltammetry indicated fairly large differences in current density between different halide salts, concentrations, cation type and pH. When comparing the absolute values of the tested aqueous solutions, it was observed current densities higher than 300 mA cm^{-2} at relative low electrode potentials (1.5 V or 1.7 were non hydrogen evolution is observed) these current densities suggest a large capacity of the solution to accept electrons. Moreover, oxidation kinetics with NaBr solutions were much higher than $ZnBr_2$ at 7 M while no large differences were observed at 2 M. This may be related to the effect that positive ions (Na^+ and Zn^+) may have an influence in halide oxidation kinetics at the large positive electrode potentials which indicated that local ionic potential effects affect the oxidation rate of the reaction. Moreover, EIS spectra seemed to go in line with this view, as there was a large resistance between $ZnBr_2$ and NaBr in the electrolyte phase transfer element. This difference is possibly related to different polybromide formation rates (for the reaction $Br^- \rightarrow Br_x^-$ + xe-). Additionally, results and literature shows that all data may be fitted by one equivalent circuit using the procedure proposed of Baukamp [30] with the fitted circuit and Nyquist plots showing the complexity of the reaction by the presence of different resistors and capacitors. Furthermore, the UV–Vis spectra showed that the Br- oxidation in aqueous solution differs considerably between pure halogen, NaBr and $ZnBr_2$.

Acknowledgment

This work was sponsored by the STW-I-Care 11854 project and Dr Ten BV, in the Netherlands as part of its ongoing battery development research and demonstration of storage systems for smart grid integration.

Appendix A. Supplementary data

Supplementary data to this article can be found online at https://doi.org/10.1016/j.seta.2019.03.001.

References

[1] Fares RL, Webber ME. Dynamic modeling of community energy storage for lifetime estimation during islanding. ECS Trans 2013;53:17–28. https://doi.org/10.1149/05307.0017ecst.
[2] Tuttle DP, Baldick R. The evolution of plug-in electric vehicle-grid interactions. IEEE Trans Smart Grid 2012;3:500–5. https://doi.org/10.1109/TSG.2011.2168430.
[3] Rothrock H. Sustainable housing: emergy evaluation of an off-grid residence. Energy Build 2014;85:287–92. https://doi.org/10.1016/j.enbuild.2014.08.002.
[4] Quintero Pulido D, Hoogsteen G, ten Kortenaar M, Hurink J, Hebner R, Smit G. Characterization of storage sizing for an off-grid house in the US and the Netherlands. Energies 2018;11:265. https://doi.org/10.3390/en11020265.
[5] Hoogsteen G, Molderink A, Hurink JL, Smit GJM. Managing energy in time and space in smart grids using TRIANA. IEEE PES Innov Smart Grid Technol Conf Eur 2015:1–6. https://doi.org/10.1109/ISGTEurope. 2014.7028973.
[6] van der Klauw T, Hurink J, Smit G. Scheduling of electricity storage for peak shaving with minimal device wear. Energies 2016;9:465. https://doi.org/10.3390/en9060465.
[7] Hoogsteen G. A cyber-physical systems perspective on decentralized energy management. University of Twente 2017. https://doi.org/10.3990/1.9789036544320.
[8] Elding LI, Gustafson L. A reaction mechanism for oxidative addition of halogen to platinum(II), reductive elimination of halide from platinum(IV) and halide assisted anations of platinum(IV) complexes. Inorganica Chim Acta 1976;19:165–71. https://doi.org/10.1016/S0020-1693(00)91090-9.
[9] Heinrich Danneel ESM. Electrochemistry theoretical electrochemistry and its physico-chemical foundations. First. New York: John Wiley & Sons; 1907.
[10] Besenhard JO. Handbook of Battery Materials. First. Austria: 1999.
[11] Cedzynska K. Properties of modified electrolyte for zinc-bromine cells. Pergamon 1995;40:971–6.
[12] Cathro KJ, Cedzynska K, Constable DC. Some properties of zinc/bromine battery. J Power Sources 1985;16:53–63.
[13] Eustace DJ. Bromine complexation in zinc-bromine circulating batteries. J Electrochem Soc 1980;127:528–32.
[14] Barnartt S, Forejt DA. Bromine-zinc secondary cells. J Electrochem Soc 1964;111:1201–4.
[15] Vafiadis H, Skyllas-kazacos M. Evaluation of membranes for the novel vanadium bromine redox flow cell. J Membrane Sci 2006;279:394–402. https://doi.org/10.1016/j.memsci.2005.12.028.
[16] Scamman DP, Reade GW, Roberts EPL, Limited RT, Station AP. Cf G. Numerical modelling of a bromide-polysulphide redox flow battery. Part 2: Evaluation of a utility-scale system. J Power Sources 2009;189:1231–9. https://doi.org/10.1016/j.jpowsour.2009.01.076.
[17] Mastragostino M, Valcher S. Polymeric salt as bromine complexing agent in a Zn-Br 2 model battery. Electrochim Acta 1983;28:501–5. https://doi.org/10.1016/0013-4686(83)85034-8.
[18] White RE, Lorimer SE. A Model of the bromine / bromide electrode reaction at a rotating disk electrode. J Electrochem Soc 1983;130:1096–103. https://doi.org/10.1149/1.2119890.
[19] Vogel I, On MA. Some problems of the zinc- bromine system as an electric energy system of higher efficiency-I. kinetics of the bromine electrode. Pergamon Press 1991;36:1403–8.
[20] Diaz MA. Thermodynamics of Cl-H2O, Br-H2O, I-H2O, Au-Cl-H2O, Au-Br-H2O and Au-I-H20 systems at 298 K. J Electroanal Chem 1993;361:13–24.
[21] Conway BE, Phillips Y, Qian SY. Surface electrochemistry and kinetics of anodic bromine formation at platinum. J Chem Soc Faraday Trans 1995;91:283–93.
[22] Heintz A, Illenberger C. Diffusion coefficients of Br 2 in cation exchange membranes. J Memb Sci 1996;113:175–81.
[23] Pell W. Zinc/bromine battery electrolytes: electrochemical, physicochemical and spectroscopic studies. Ottawa: Ottawa University; 1994.
[24] Walter S, Aym D, Walter S, Gabelica Z, Valange S. Evaluation of carbon cryogels used as cathodes for non-flowing zinc – bromine storage cells zinc – bromine storage. Cells 2008. https://doi.org/10.1016/j.jpowsour.2007.09.076.
[25] Faita G, Fiori G, Mussini T. Electrochemical processes of the bromine/ bromide system. Electrochim Acta 1968;13:1765–72. https://doi.org/10.1016/0013-4686(68)80084-2.
[26] Bennett B, Chang J, Bard AJ. Mechanism of the Br-/Br2 redox reaction on platinum and glassy carbon electrodes in nitrobenzene by cyclic voltammetry. Electrochim Acta 2016;219:1–9. https://doi.org/10.1016/j.electacta.2016.09.129.
[27] Kolthoff IM, Coetzee JF. Polarography in acetonitrile. II. Metal ions which have

significantly different polarographic properties in acetonitrile and in water. Anodic waves. Voltammetry at rotated platinum electrode. J Am Chem Soc 1957;79:1852–8. https://doi.org/10.1021/ja01565a023.
[28] Duhlev R, Brown ID, Faggiani R. IUCr. Zinc bromide dihydrate ZnBr 2.2H2O: a double-salt structure. Acta Crystallogr Sect C Cryst Struct Commun 1988;44:1696–8. https://doi.org/10.1107/S0108270188006584.
[29] Haaf WR, Carpenter GB. IUCr. The crystal structure of sodium bromide dihydrate. Acta Crystallogr 1964;17:730–2. https://doi.org/10.1107/S0365110X64001797.
[30] Boukamp BA. a Package for Impedance/Admittance Data Analysis. Solid State Lonics 2014;18(19):1–5. https://doi.org/10.1007/s13398-014-0173-7.2.
[31] Boukamp BA. A linear Kronig-Kramers transform test for immittance data validation. J Electrochem Soc 1995;142:1885–94. https://doi.org/10.1149/1.2044210.
[32] Boukamp BA. A nonlinear least squares fit procedure for analysis of immittance data of electrochemical systems. Solid State Ionics 1986;20:31–44. https://doi.org/10.1016/0167-2738(86)90031-7.
[33] Boukamp BA. Electrochemical impedance spectroscopy in solid state ionics: Recent advances. Solid State Ionics 2004;169:65–73. https://doi.org/10.1016/j.ssi.2003.07.002.
[34] Arai K, Kusu F, Noguchi N, Takamura K, Osawa H. Selective determination of chloride and bromide ions in serum by cyclic voltammetry. Anal Biochem 1996;113:109–13.
[35] Chen M, Huang S, Hsieh C, Lee J-Y, Tsai T. Electrochimica acta development of a novel iodine-vitamin C/vanadium redox flow battery. Electrochim Acta 2014;141:241–7. https://doi.org/10.1016/j.electacta.2014.07.069.
[36] Simonet V, Calzavara Y, Hazemann JL, Argoud R, Geaymond O, Raoux D. Structure of aqueous ZnBr 2 solution probed by X-ray absorption spectroscopy in normal and hydrothermal conditions. J Chem Phys 2002;116:2997–3006. https://doi.org/10.1063/1.1433499.
[37] Omta AW, Kropman MF, Woutersen S, Bakker HJ. Negligible Effect of Ions on the Hydrogen-Bond Structure in Liquid Water. Science (80-) 2003;301:347–9. https://doi.org/10.1126/science.1084801.
[38] Lin Y-S, Auer BM, Skinner JL. Water structure, dynamics, and vibrational spectroscopy in sodium bromide solutions. J Chem Phys 2009;131:144511https://doi.org/10.1063/1.3242083.
[39] Adanuvor PK, White RE, Lorimer SE. The effect of the tribromide complex reaction on the oxidation/reduction current of the Br 2 / Br − electrode. J Electrochem Soc 1987;134:1450–4. https://doi.org/10.1149/1.2100688.
[40] Mastragostino M, Gramellini C. Kinetic study of the electrochemical processes of the bromine/bromine aqueous system on vitreous carbon electrodes. Electrochim Acta 1985;30:373–80. https://doi.org/10.1016/0013-4686(85)80198-5.
[41] Park S, Shin S, Jung D, Chae J, Chang J. Understanding Br− transfer into electrochemically generated discrete quaternary ammonium polybromide droplet on Pt ultramicroelectrode. J Electroanal Chem 2017;797:97–106. https://doi.org/10.1016/j.jelechem.2017.05.014.
[42] Izumi I, Sato J, Iwashita N, Inagaki M. Electrochemical intercalation of bromine into graphite in an aqueous electrolyte solution. Synth Met 1995;75:75–7.
[43] Gaier JR, Ditmars NF, Dillon AR. Aqueous electrochemical intercalation of bromine into graphite fibers. Carbon N Y 2005;43:189–93. https://doi.org/10.1016/j.carbon.2004.09.005.
[44] Bell JG, Wang J. Current and potential oscillations during the electro-oxidation of bromide ions. J Electroanal Chem 2015;754:133–7. https://doi.org/10.1016/j.jelechem.2015.07.016.